

Effect of planetary ball milling process parameters on the nitrogen adsorption properties of multiwall carbon nanotubes

Ibolya Zita Papp · Gábor Kozma · Róbert Puskás ·
Tímea Simon · Zoltán Kónya · Ákos Kukovecz

Received: 5 December 2012 / Accepted: 31 January 2013 / Published online: 12 February 2013
© Springer Science+Business Media New York 2013

Abstract The dependence of multiwall carbon nanotube (MWCNT) length distribution and some nitrogen derived morphological descriptors on various planetary ball milling process parameters was investigated. Ball milling was found to cut nanotubes into smaller pieces, narrow their length distribution and increase their specific surface area and surface fractal dimension. Typical length reduction was from 1300 to 200 nm, specific surface area increase from 160 to 340 m²g⁻¹ and surface fractal dimension increase from 2.47 to 2.70. The pore size distribution of pristine MWCNTs exhibited a mesoporous character dominated by intertube channels. A sharp maximum appeared at $d = 3.6$ nm diameter when the milling power was increased. This increase was attributed to the opening of intratube voids. Processes involving graphitic platelet detachment, tube wall amorphization or carbonaceous debris accumulation appear to play only minor roles under the studied experimental conditions of planetary milling. Control over the morphology of the milled material is best achieved by varying the diameter and the mass ratio of the grinding balls as well as the classical process parameters like disk rotational speed, milling time and number of balls.

Keywords Carbon nanotube · Ball mill · Nitrogen adsorption · Fractal dimension

1 Introduction

Multiwall carbon nanotubes (MWCNTs) consist of coaxially stacked cylindrical graphene sheets capped by half fullerenes at both ends. They feature a hollow internal channel with a diameter of 3–6 nm, a typical outer diameter between 10–30 nm and lengths above 1 micrometer (Iijima 1991). Their excellent electrical and thermal conductivity, high stiffness and axial strength have attracted lots of attention from the scientific community in the past two decades (Kavan et al. 2004; Zubizarreta et al. 2008; Munoz et al. 2010). The wholesale price of MWCNTs has recently dropped below 200 USD/kg and therefore, carbon nanotubes are no longer merely objects of scientific interest but a raw material for the production industries. Consequently, it is important to expand the toolset of materials science with methods capable of tailoring the properties of MWCNTs in a cheap and scalable way.

Solid state transformations are important in several fields of technological chemistry including ceramics synthesis and catalyst support manufacture (Kiss and Boskovic 2012). In particular, ball milling is used by several industries including ceramics, paint manufacturing, pharmaceuticals and construction. Variants of the ball milling process have been previously applied to modify the length (Pierard et al. 2001; Kim et al. 2002), particle size distribution (Wang et al. 2003) hydrogen adsorption properties (Liu et al. 2003) and lithium intercalation capacity (Gao et al. 2000) of carbon nanotubes as well as to perform carbon nanoparticle synthesis (Li et al. 1999). Planetary ball milling is particularly suitable for improving the

I. Z. Papp · G. Kozma · R. Puskás · T. Simon · Z. Kónya ·
Á. Kukovecz (✉)
Department of Applied and Environmental Chemistry,
University of Szeged, Rerrich Béla tér 1, Szeged 6720, Hungary
e-mail: kakos@chem.u-szeged.hu

Z. Kónya
MTA-SZTE Reaction Kinetics and Surface Chemistry Research
Group, Rerrich ter 1, Szeged 6720, Hungary

Á. Kukovecz
MTA-SZTE “Lendület” Porous Nanocomposites Research
Group, Rerrich ter 1, Szeged 6720, Hungary

dispersion of MWCNTs in aluminum (Esawi et al. 2009; Nouni et al. 2012) and polymer matrices. Despite its many applications and high potential for serving as an industrially feasible technology for nanotube property tailoring (Kukovecz and Konya 2008), a generally accepted model describing all energy transfers happening during the milling of carbon nanotubes is not yet available. However, attempts have been made to describe the energetics of high-energy milling (Abdellaoui et al. 1996; Watanabe et al. 1995; Huang et al. 1997) and planetary ball milling (Chattopadhyay et al. 2001) in general.

Our goal in this contribution is to provide experimental data that can support further model development work in the field. In particular, we report the dependence of average multiwall nanotube length, specific surface area, pore size distribution and surface fractal dimension on the most important process parameters of a planetary ball mill. These morphological descriptors were determined by transmission electron microscopy (TEM) image analysis and nitrogen adsorption isotherm analysis. Carefully controlled and described experimental conditions facilitate the reproduction of the reported results.

2 Experimental

2.1 Carbon nanotube synthesis

Multiwall carbon nanotubes were synthesized by our previously described catalytic chemical vapor deposition (CCVD) method (Kukovecz et al. 2000). A MgO support is first impregnated with 2.5–2.5 weight % Co and Fe precursor from the aqueous solution of the respective acetate salts. This catalyst is then annealed in N₂ flow for 1 h in a preheated horizontal tube reactor at 973 K and finally, acetylene is mixed into the gas flow to initiate to synthesis of multiwall carbon nanotubes over the Fe–Co/MgO catalyst at 973 K. After 1 h of CCVD reaction time the system is allowed to cool down to room temperature in N₂ flow.

The catalyst is then removed by leaching in hydrochloric acid and the product is washed to pH 7 and dried in air. This procedure yields multiwall carbon nanotubes of good quality with a typical length of 1–1.3 μm and a typical diameter of 30 nm.

2.2 Ball milling experiments

Ball milling experiments were performed in a Fritsch Pulverisette 6 planetary ball mill which allows very precise control over all relevant process parameters. 0.5 g MWCNT material was milled in a 80 mL stainless steel drum at room temperature in air atmosphere in each experiment. Parameters to be varied were identified on the basis of our previous experience with nanotube grinding (Kukovecz et al. 2005). Thus, the six experiment series detailed in Tables 1 and 2 were performed. The planetary mill disk rotation speed was varied from 150 to 600 rpm (Table 1A), the milling time from 5 to 60 min (Table 1B), the number of 10 mm balls from 5 to 25 (Table 1C), the number of 5 mm balls from 40 to 200 and (Table 1D) the mass ratio of large to small balls from 10:1 to 1:10 (Table 1E and Table 2). The mass of one 10 mm diameter ball was 4.0 g and that of a 5 mm one was 0.5 g. Only one parameter was varied in each series while the others were kept constant (see Table 1) to facilitate comparison between the different series.

2.3 Sample characterization

All samples were sonicated in an Elmesonic-S80H type ultrasonic unit at 37 kHz frequency for 15 min in ethanol after milling to separate MWCNTs and subsequently dried at 353 K in air before the nitrogen adsorption measurement. Transmission Electron Microscope (TEM) images were recorded on a FEI Tecnai G² 20 X-TWIN instrument with a point resolution of 0.26 nm. Diluted suspensions of the MWCNT samples in ethanol were drop-dried on holey carbon coated copper TEM grids. At least five TEM

Table 1 Overview of the milling process parameters varied in this study

	Milling series				
	A	B	C	D	E
W_d (rpm)	150, 200, 250, 300, 350, 400, 450, 500, 550, 600	350	350	350	350
t (min)	60	5, 10, 15, 20, 25, 30, 35, 40, 45, 50, 55, 60	60	60	60
N_b (pcs)	15	15	5, 10, 15, 20, 25	40, 80, 120, 160, 200	See Table 2.
d_b (mm)	10	10	10	5	5&10

W_d is the rotational speed of the main disc in rpm, t is the milling time in minutes, N_b is the number of balls, d_b is the diameter of grinding balls in mm

Table 2 Details of the large to small ball ratio variation experiments (see Table 1E for the other process parameters)

Sample	1	2	3	4	5	6	7	8	9
Ratio of ball's mass	1:0	10:1	4:1	2:1	1:1	1:2	1:4	1:10	0:1
N_b of 10 mm ball (pcs)	15	14	12	10	8	5	3	1	0
N_b of 5 mm ball (pcs)	0	8	24	40	60	80	96	112	120

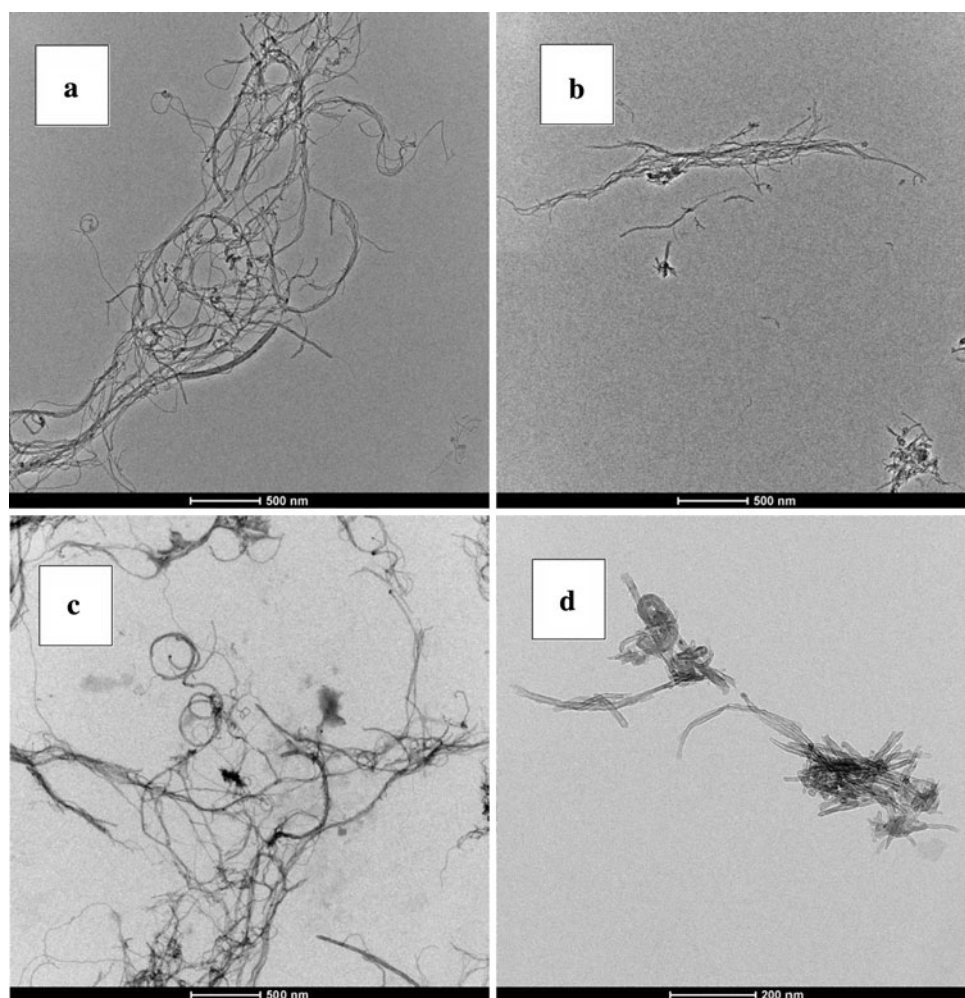
micrographs were recorded for each sample at each relevant magnification. The length distribution data was derived by TEM image analysis performed using the ImageJ software. The length of at least 100 nanotubes was measured for each data point. Nitrogen adsorption isotherms were recorded at 77 K using a QuantaChrome Nova 2000 surface area analyzer. Before the measurement the samples were outgassed at 423 K for 1 h to remove any adsorbed contaminants. The specific surface areas (A_s^{BET}) were calculated using the multipoint BET method on the

basis of six data points of the adsorption isotherms near monolayer coverage. Pore size distribution (PSD) curves were calculated from the desorption branch of the isotherms using the Barrett-Joyner-Halenda (BJH) method (Barrett et al. 1951). Surface fractal dimension (D_s) was calculated using the Frenkel-Halsey-Hill (FHH) method (Pfeifer et al. 1989) from adsorption data near monolayer coverage (Tang et al. 2003).

3 Results and discussion

Planetary ball milling of the multiwall carbon nanotube starting material invariably resulted in an increase in the apparent density of the material. On the basis of earlier low-impact milling studies this suggests that the nanotubes were cut into smaller pieces corresponding to a more compact macroscopic structure. The morphology of this material was studied in detail by TEM and nitrogen adsorption analysis. The detailed parameters of the discussed milling series are listed in Tables 1 and 2.

Fig. 1 Characteristic TEM images of the carbon nanotubes subjected to various milling treatments. Images corresponding to series A 150 and 350 rpm are depicted in (a) and (b), respectively. c, d are typical for series B 5 min (c) and 60 min (d) experiments, respectively



3.1 MWCNT length distribution analysis

Characteristic TEM images illustrating the changes suffered by the nanotubes upon milling are depicted in Fig. 1. Increasing either the rotational speed of the planetary mill disk (Fig. 1a, b) or the duration of the milling (Fig. 1c, d) both yield shorter nanotubes. The apparent diameter of the tubes is unaffected by the milling and no amorphous carbon debris formation can be observed.

The average nanotube length was determined after each milling experiment by TEM image analysis. The resulting histograms are depicted in Fig. 2 for the A series. Continuous lines in this figure denote normal distribution probability density function fits to the measured data. The fitted mean length and standard deviation are (904; 431), (530; 309), (179; 112) and (89; 57) nm for samples milled at 150, 250, 400 and 550 rpm, respectively. It is interesting to note that besides reducing the average nanotube length, ball milling narrowed the length distribution as well. Although this might appear counter-intuitive at first for a purely stochastic process as milling, it is actually quite understandable when considering that longer nanotubes are more likely to suffer an impact than shorter ones. Therefore, the more impacts occur during the process, the more will any deviations from the average length cancel out.

Average MWCNT length as a function of various milling parameters is depicted in Fig. 3. The cutting effect was most pronounced in the A series as evidenced by the

reduction of average nanotube length from 942 nm (150 rpm) to 88 nm (600 rpm) in an inversely proportional relationship. It is interesting that a similar general trend is observable in Fig. 3b where the effect of milling time at a constant 350 rpm rotational speed is studied. The sharp initial drop in average nanotube length is attributed to the breaking of the longest nanotubes into two parts at defect sites. From this point onwards, length reduction is again proportional with milling time. This is a non-trivial finding because rotational speed and milling time actually control very different parameters, namely, the energy and the number of ball hits, respectively. The final nanotube length achieved in this series matches the corresponding (350 rpm) result of the previous (A) series well. Figures 3c, d characterize the nanotube length reduction as a function of the number of large (series C) and small (series D) balls, respectively. It is well-known in mechanochemistry that the milling time and the number of balls used are strongly correlated process variables because they both control the number of hits experienced by the milled material. Therefore, the length decrease tendency observed in Fig. 3c agrees well with the expectations based on Fig. 3b results. Further confirmation is provided by Fig. 3d which depicts the gentle cutting of MWCNTs by a large number of small milling balls. Both Fig. 3c, d indicate that changing the number of milling balls offers better control over nanotube length than changing the milling time. Therefore, varying the number and diameter of the milling

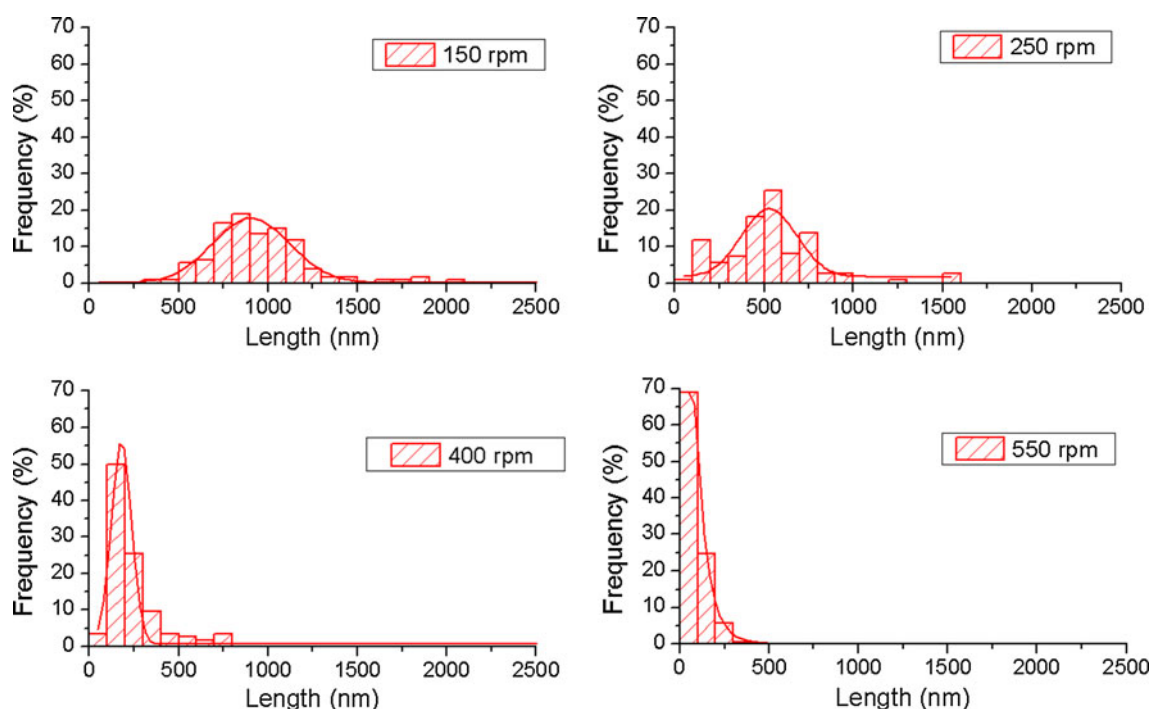


Fig. 2 Average length distributions of ball milled MWCNT samples from series A. The continuous line denotes a normal distribution fitted to the experimental data

balls is an adequate method to tune the average nanotube length to the desired size range.

Series E was run to confirm the hypothesis that mixtures of large and small diameter balls would combine the beneficial cutting effects of both types and provide even better control over MWCNT length distribution. In these experiments the total weight of balls was kept at a constant of 60 g per experiment while the weight ratio of the large and small balls was scanned from 10:1 to 1:10. Curiously, the experimental results depicted in Fig. 3e confuted our hypothesis and revealed that the average nanotube length is almost constant at 760 nm regardless of the ball mixture loading (see Fig. 3e; Tables 1 and 2 as well). Since larger balls transfer more energy upon impact than smaller ones at

the same rotational speed, we may conclude here that the individual impact energy and the total number of hits are also strongly correlated process parameters. The same overall length reduction ratio can be reached by using a few larger or several smaller balls provided that the total ball mass and rotational speed are kept constant.

3.2 Nitrogen adsorption analysis

Nitrogen adsorption isotherms measured at 77 K provide three important morphological descriptors: the specific surface area (A_s^{BET}) which characterizes the overall surface of the sample available for nitrogen adsorption, the empirical pore diameter distribution function (PSD curve)

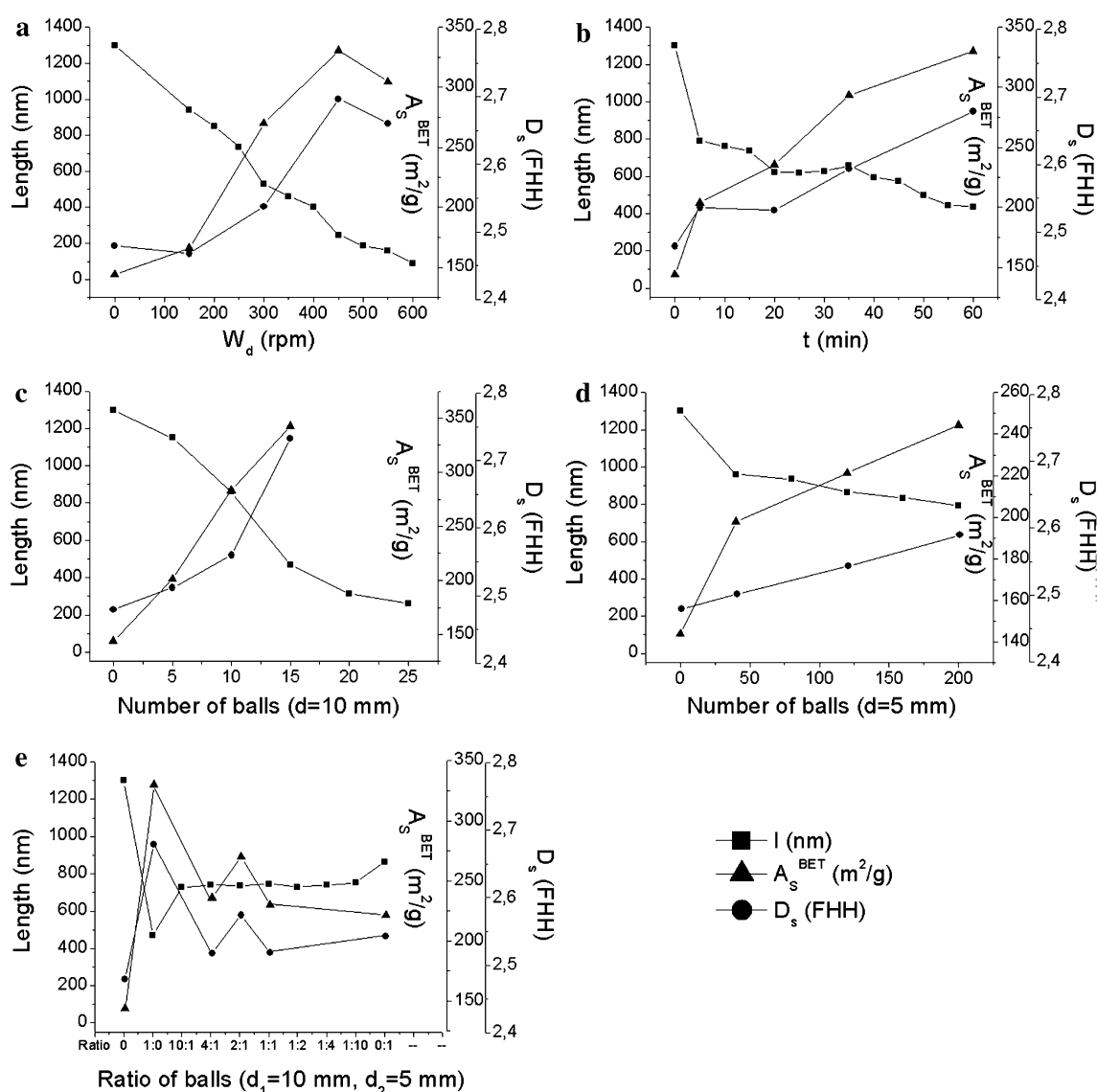


Fig. 3 Average multiwall carbon nanotube length (*square*), specific surface area (*triangle*) and surface fractal dimension (*circle*) as a function of disk rotation speed (a), milling time (b), number of large balls (c), number of small balls (d) and total mass ratio of large balls to small balls (e)

which describes the porosity of the material and the surface fractal dimension (D_s) which monitors the self-similarity of the surface (Rigby et al. 2008). Ideal geometrical objects exist in integer dimensions, for example zero dimensional points, one dimensional lines and curves, two dimensional plane figures like circles and squares and three dimensional solid objects. However, most real material surfaces are described better by the non-integer dimension D_s falling between two integer values because of the irregularity of their surface. In the case of multiwall carbon nanotubes, D_s can be interpreted as a measure of deviation from the ideal cylindrical surface because of local defects, wells, carbonaceous debris deposits etc.

Characteristic N_2 adsorption-desorption isotherms of samples milled at three different rotational speeds are depicted in Fig. 4. The fundamentals of the adsorption process are not affected by the milling insofar as all three curves are Type II isotherms according to the IUPAC classification. Differences between the isotherms are related to the effect of nanotube cutting on the specific surface area and to the changes occurring in the macroporous capillary condensation region. A detailed quantitative analysis of all isotherms was performed and the results were summarized in Fig. 3. The right-hand side axes in the plots of Fig. 3 give the A_s^{BET} and the D_s values as a function of milling process parameters. The starting MWCNT material had a specific surface area of $180 \text{ m}^2\text{g}^{-1}$ and surface fractal dimension of 2.47, both of which are typical values for this material as confirmed by earlier reports (Kanyó et al. 2004). It should be noted here that multiwall carbon nanotubes grow “closed”, that is, their hollow interior is inaccessible from the outside after synthesis because of the half fullerene caps terminating the tubular structure.

Length reduction in the planetary ball mill invariably resulted in materials with higher specific surface area (up to $340 \text{ m}^2\text{g}^{-1}$) and a significant increase in surface fractal dimension (above 2.70). Since the specific surface area measures the amount of primary adsorption sites, this indicates that the morphology of the material underwent major changes. The increasing specific surface area could originate either from the opening of the MWCNTs during milling or from the partial demolition of the nanotube walls into a graphitic carbon platelets. Although the TEM images (Fig. 1) suggest that the former explanation is probably more valid, a more detailed analysis was necessary. First of all, let us note that regardless of the milling series, specific surface area and surface fractal dimension curves in Fig. 3a–e always follow the same trend, indicating a strong positive correlation between these two descriptors. This is important because graphitic platelets removed by milling would increase the surface area but simultaneously decrease the surface fractal dimension by introducing

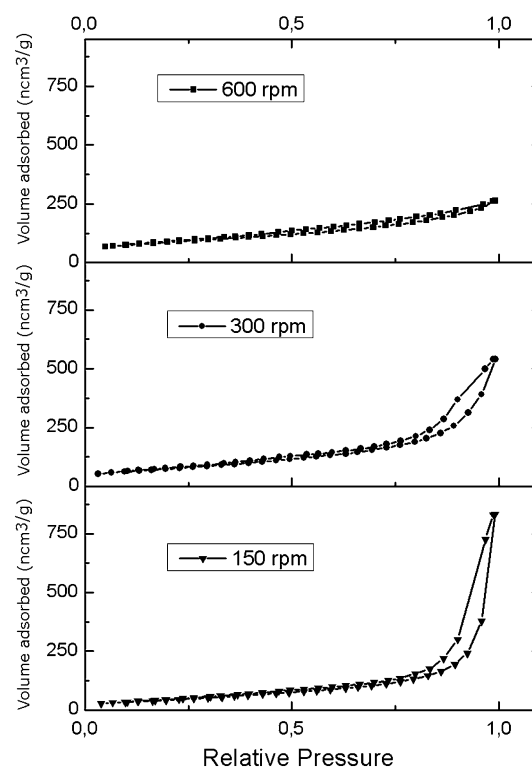


Fig. 4 Characteristic N_2 adsorption–desorption isotherms recorded at 77 K on Series A samples milled at 150, 300 and 600 rpm

completely flat surfaces into the material. On the other hand, opening the inner channel of the nanotubes for adsorption increases the dimensional depth of the material which would be measured as an increase in D_s . Secondly, observe that A_s^{BET} and the D_s values corresponding to the same average nanotube length are very similar in all the milling series involving large diameter balls (Fig. 3a–c) but different and typically smaller for the cases involving small balls (Fig. 3d–e). A possible interpretation for this is that the smaller milling balls are less efficient in making the nanotube interior available for nitrogen adsorption and therefore, the morphology of the cut nanotubes in these cases is more similar to that of the starting material. Finally, it should be noted here that the available experimental evidence is not sufficient to unambiguously exclude the possibility of carbonaceous debris effects on the specific surface area and surface fractal dimension at the most severe milling conditions.

The pore size distribution (PSD) curves of series A and B are presented in Fig. 5a, b, respectively. Here, “pore radius” refers to the radius of equivalent cylindrical pores which release nitrogen at a particular relative pressure as defined by the Kelvin equation and calculated by the BJH method. The pore structure of the starting material is typical for a pristine MWCNTs matrix which has a primarily mesoporous character without any preferred pore diameters

except the intertube channels indicated by the upward curvature of the PSD function at the lowest radii. Samples subjected to the mildest milling action (150 rpm or 5 min) are similar to the starting material. A new maximum appears in the PSD curve upon more severe ball impacts at approx. 3.6 nm pore diameter which is a typical MWCNT inner channel diameter value according to previous HRTEM studies. Although macroscopic amounts of multiwall carbon nanotubes always feature a certain distribution of both inner and outer tube diameters, it appears reasonable to assume on the basis of the TEM and N_2 adsorption evidence that the PSD maximum emerges because of the nanotube interiors becoming available for adsorption. Comparing these plots with the corresponding nanotube length and specific surface area data in Fig. 3a, b reveals that the appearance of the PSD maximum coincides with the marked increase in specific surface area and surface fractal dimension. This phenomenon is in agreement with the TEM observations and strongly supports the tube opening hypothesis instead of the wall amorphization hypothesis.

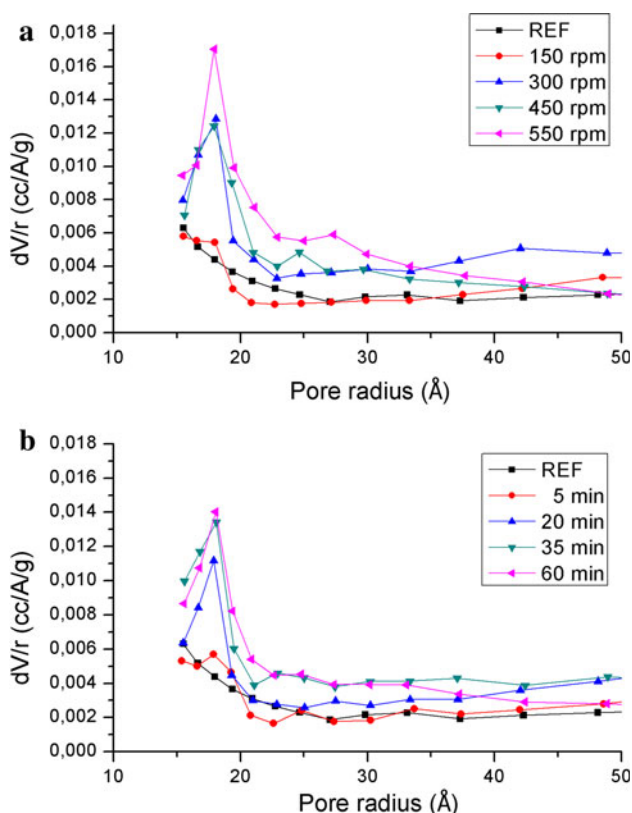


Fig. 5 Pore size distribution (PSD) curves of the milled MWCNT samples, calculated from the desorption branch of the N_2 desorption isotherm using the BJH method. **a** depicts results derived from series “A” data and **b** corresponds to measurements in the series “B”. The “REF” curve identifies the data of the unmilled starting MWCNT material

4 Conclusions

The dependence of multiwall carbon nanotube length distribution and nitrogen adsorption isotherm derived morphological descriptors on various planetary ball milling process parameters was investigated. Ball milling was found to cut nanotubes into smaller pieces, narrow their length distribution and increase their specific surface area and surface fractal dimension. The results helped us conclude that the main reason behind the increasing specific surface area of planetary ball milled MWCNTs is that the interior becomes accessible for nitrogen adsorption upon nanotube cutting, whereas processes involving graphitic platelet detachment, tube wall amorphization or carbonaceous debris accumulation may play only inferior roles. Our study also revealed that the rotational speed of the planetary ball mill, the milling time and the number of balls used are strongly correlated process parameters. Varying the diameter and the mass ratio of the grinding balls allows the fine tuning of the nanotube cutting process because smaller balls are less effective in opening the MWCNTs but offer more control over the average length of the final milled product.

Acknowledgments The financial support of the OTKA 106234, TÁMOP-4.2.2.A-11/1/KONV-2012-0047 and TÁMOP-4.2.2.A-11/1/KONV-2012-0060 Projects and the EC FP7 INCO “NAPEP” network is acknowledged.

References

- Abdellaoui, M., Rahouadj, R., Gaffet, E.: Optimisation of the mechanical shock transfer in a modified horizontal rod mill. *Mater. Sci. Forum* **225**, 255–260 (1996)
- Barrett, E.P., Joyner, L.G., Halenda, P.P.: The determination of pore volume and area distributions in porous substances. I. Computations from nitrogen isotherms. *J. Am. Chem. Soc.* **73**, 373–380 (1951)
- Chattopadhyay, P.P., Manna, I., Talapatra, S., Pabi, S.K.: A mathematical analysis of milling mechanics in a planetary ball mill. *Mater. Chem. Phys.* **68**, 85–94 (2001)
- Esawi, A.M.K., Morsi, K., Sayed, A., Gawad, A.A., Borah, P.: Fabrication and properties of dispersed carbon nanotube-aluminum composites. *Mater. Sci. A* **508**, 167–173 (2009)
- Gao, B., Bower, C., Lorentzen, J.D., Fleming, L., Kleinhammes, A., Tang, X.P., et al.: Enhanced saturation lithium composition in ballmilled single-walled carbon nanotubes. *Chem. Phys. Lett.* **327**, 69–75 (2000)
- Huang, H., Pan, J., McCormick, P.G.: Prediction of impact forces in a vibratory ball mill using an inverse technique. *Int. J. Impact Eng.* **19**, 117–126 (1997)
- Iijima, S.: Helical microtubules of graphitic carbon. *Nature* **354**, 56–58 (1991)
- Kanyó, T., Kónya, Z., Kukovecz, A., Berger, F., Dékány, I., Kiricsi, I.: Quantitative characterization of hydrophilic-hydrophobic properties of MWNTs surfaces. *Langmuir* **20**, 1656–1661 (2004)
- Kavan, L., Dunsch, L., Kataura, H.: Electrochemical tuning of electronic structure of carbon nanotubes and fullerene peapods. *Carbon* **42**, 1011–1019 (2004)

- Kim, Y.A., Hayashi, T., Fukai, Y., Endo, M., Yanagisawa, T., Dresselhaus, M.S.: Effect of ball milling on morphology of cupstacked carbon nanotubes. *Chem. Phys. Lett.* **355**, 279–284 (2002)
- Kiss, E.E., Boskovic, G.C.: Impeded solid state reactions and transformations in ceramic catalysts supports and catalysts. *Process Appl Ceram* **6**, 173–182 (2012)
- Kukovecz, A., Konya, Z.: Mechanichemistry of carbon nanotubes. In: Basiuk, V.A. (ed.) *Chemistry of carbon nanotubes*, pp. 237–254. American Scientific Publishers, Cambridge (2008)
- Kukovecz, A., Konya, Z., Naragaju, N., Willems, I., Tamasi, A., Fonseca, A., Nagy, J.B., Kiricsi, I.: Catalytic synthesis of carbon nanotubes over Co, Fe and Ni containing conventional and sol-gel silica-aluminas. *Phys. Chem. Chem. Phys.* **2**, 3071–3076 (2000)
- Kukovecz, A., Kanyó, T., Kónya, Z., Kiricsi, I.: Long-time low-impact ball milling of multiwall carbon nanotubes. *Carbon* **43**, 994–1000 (2005)
- Li, Y.B., Wei, B.Q., Liang, J., Yu, Q., Wu, D.H.: Transformation of carbon nanotubes to nanoparticles by ball milling process. *Carbon* **37**, 493–497 (1999)
- Liu, F., Zhang, X., Cheng, J., Tu, J., Kong, F., Huang, W., et al.: Preparation of short carbon nanotubes by mechanical ball milling and their hydrogen adsorption behavior. *Carbon* **41**, 2527–2532 (2003)
- Munoz, E., Ruiz-Gonzalez, M.L., Seral-Ascaso, A., Sanjuan, M.L., Gonzalez-Calbet, J.M., Laguna, M., de la Fuente, G.F.: Tailored production of nanostructured metal/carbon foam by laser ablation of selected organometallic precursors. *Carbon* **48**, 1807–1814 (2010)
- Nouni, N., Ziaei-Rad, S., Adibi, S., Karimzadeh, F.: Fabrication and mechanical property prediction of carbon nanotube reinforced Aluminum nanocomposites. *Mater. Des.* **34**, 1–14 (2012)
- Pfeifer, P., Wu, Y.J., Cole, M.W., Krim, J.: Multilayer adsorption on a fractally rough surface. *Phys. Rev. Lett.* **62**, 1997–2000 (1989)
- Pierard, N., Fonseca, A., Konya, Z., Willems, I., Van Tendeloo, G., B.Nagy, J.: Production of short carbon nanotubes with open tips by ball milling. *Chem. Phys. Lett.* **335**, 1–8 (2001)
- Rigby, S.P., Chigada, P.I., Perkins, E.L., Watt-Smith, M.J., Lowe, J.O., Edler, K.J.: Fundamental studies of gas sorption within mesopores situated amidst an inter-connected, irregular network. *Adsorption* **14**, 289–307 (2008)
- Tang, P., Chew, N.Y.K., Chan, H.K., Raper, J.A.: Limitations of determination of surface fractal dimension using N₂ adsorption isotherms and modified Frenkel–Halsey–Hill theory. *Langmuir* **19**, 2632–2638 (2003)
- Wang, Y., Wu, J., Wei, F.: A treatment method to give separated multi-walled carbon nanotubes with high purity, high crystallization and a large aspect ratio. *Carbon* **41**, 2939–2948 (2003)
- Watanabe, R., Hashimoto, H., Lee, G.G.: Computer-simulation of milling ball motion in mechanical alloying. *Mater. Trans. JIM* **36**, 102–109 (1995)
- Zubizarreta, L., Gomez, E.I., Arenillas, A., Ania, C.O., Parra, J.B., Pis, J.J.: H₂ storage in carbon materials. *Adsorption* **14**, 557–566 (2008)